Dynamic properties of neutral excitations produced in electron-bombarded superfluid helium. II. Afterglow fluorescence of excited helium molecules*

J. W. Keto,† F. J. Soley, M. Stockton,‡ and W. A. Fitzsimmons
University of Wisconsin, Madison, Wisconsin 53706
(Received 3 April 1974)

We have investigated the time dependence of the afterglow emission of pulsed-electron–bombarded superfluid helium, and in addition we have studied the effects of pressure on the steady-state intensities of the atomic and molecular emissions of the excited liquid. Our results indicate that two distinct mechanisms populate the excited states in the liquid. The first production mechanism basically determines the steady-state properties of the excited liquid and it is responsible for the rapid initial decay of the fluorescence during the first 10^{-8} sec of the afterglow. This rapid decay time taken with the observed exponential decrease of the steady-state intensities with increasing pressure indicates that most of the excited states are nonradiatively quenched by the surrounding ground-state liquid. The second production mechanism results in a slowly decaying late afterglow fluorescence of the excited liquid. It is shown that this late time emission is due to the bilinear destruction of the long-lived $He_2(a\,^3\Sigma_u^+)$ metastable molecules which are produced also in the liquid by the electrons. It is shown further that most of the energy released during these bilinear reactions results in the population of the $He_2(A\,^1\Sigma_u^+)$ state which subsequently radiates in the vacuum-ultraviolet region of the spectrum.

I. INTRODUCTION

The scintillation of superfluid helium when subjected to energetic particle bombardment has been the subject of considerable recent investigation. The α-particle–induced scintillation of liquid helium was reported first by Moss and Hereford in 1963.[1] Shortly thereafter Jortner *et al.* provided evidence of neutral electronic excitations in condensed helium by observing the enhanced emission of oxygen and nitrogen impurities when the liquid is subjected to α-particle bombardment.[2] The more recent experiments of Surko and Reif established the existence of long-lived but unidentified excitations in superfluid helium.[3] The question of identifying the nature of the electronic excitations of the liquid remained unanswered until 1969 when Dennis *et al.* noted that a much greater intensity of emission could be achieved by using an electron beam to excite the liquid.[4] These authors made direct spectroscopic measurements of the liquid-helium fluorescence and established that under electron bombardment the visible and near-infrared emission was due to excited states of the neutral diatomic helium molecule, with some emission coming from excited atoms. In 1970, Stockton *et al.* and Surko *et al.* simultaneously reported the first vacuum uv spectrum of electron-bombarded superfluid helium, and it was shown that this emission resulted from the radiative dissociation of the $He_2(A\,^1\Sigma_u^+)$ molecule.[5,6] Further investigation showed that the uv fluorescence accounted for over 99% of the total scintillation intensity.[7]

We, as well as others, have believed that the transient or time-dependent behavior of the liquid-helium fluorescence should provide information about the mechanisms for the production and destruction of the excited states in the liquid. For example, several experimenters have investigated the shape of uv scintillation pulses coming from single α-particle tracks.[8] Unfortunately, it is difficult to correlate these observations with particular excited states of the liquid since the emission spectrum of α-particle–excited superfluid helium has not been reported.

On the other hand, both the optical emission and absorption spectra of electron-beam–excited liquid helium are now reasonably well known.[4,9] Furthermore, the experiments described in Paper I of this report have established the dynamic behavior of the spin-triplet metastable states of helium which are produced in the liquid.[10] Thus in the case of electron bombardment there is a large body of information which may be expected to be related to the time dependence of the electron-induced fluorescence of the liquid. Furthermore, the enchanced intensity of emission which results from using an electron beam makes it possible to study the transient behavior of individual molecular emission bands. For example, it is shown in this paper that there are two distinctly different mechanisms which populate the excited molecular states in liquid helium. One mechanism is observed to be very prompt since most of the fluorescence is produced within a time that is of the order or less than 10^{-8} sec after the impinging

electrons. This fast transient response time and the observed decrease of the steady-state intensities with increasing pressure indicates that most of the excited states are nonradiatively quenched by the surrounding superfluid. The second populating mechanism may be described as slow since under our experimental conditions the characteristic times are of the order of milliseconds. It is shown that this second mechanism is due to the bilinear destruction of the metastable helium molecules, and further that most of the energy released by this process results in the formation of $He_2(A\,^1\Sigma_u^+)$ molecules.

II. EXPERIMENTAL PROCEDURE

In these experiments we observe the steady-state intensity as well as the decay in the intensity of the major visible, infrared, and vacuum-uv molecular emission bands of superfluid helium when bombarded with repetitive pulses of 160-keV electrons. The emission spectrum of electron-beam–excited superfluid helium and a diagram showing the molecular transitions monitored during these experiments is shown in Fig. 1. The visible and infrared spectrum is essentially identical to that previously reported by Dennis *et al.* The uv spectrum is taken from the work of Stockton *et al.*[4,5] The details of the electron accelerator, the method of sample preparation and temperature regulation, and the method of pulsing the electron beam, with 10 to 90% rise and fall times of 10 and 20 nsec, respectively, have been published elsewhere.[5] The optical arrangement used to study the visible and infrared emissions bands is shown schematically in Fig. 2. A $\frac{1}{2}$-m Jarrel Ash spectrometer with a bandpass of about 13 Å was used to isolate most of the visible and infrared emission bands for individual study; a narrow bandpass interference filter was used to isolate the intense 10 400-Å $d^3\Sigma_u^+ \rightarrow c^3\Sigma_g^+$ band. The entire optical detection system, including the collection lens, precision f-stops, spectrometer, and detector, was mounted on a pivoted optical bench so that the system could be rotated quickly and accurately in order to alternately observe equal surface areas of either the excited liquid or a radiance standard strip lamp. This procedure minimized the errors in the measurements of absolute intensity introduced by the slowly varying time-dependent sensitivity of the cooled photomultipliers. Cooled EMI 9558 (S-20) and FW 118 (S-1) photomultipliers served as detectors for the visible and infrared, and the faster but less sensitive RCA 7102 (S-1) was used when faster response times were necessary. The uv emission was studied using a concave grating vacuum-uv spectrometer which forms an integral part of the sample chamber and liquid helium Dewar. This particular spectrometer is described elsewhere.[5] The uv continuum was studied in zeroth order (using the grating as a mirror) and at the wavelengths of 736 and 862 Å with a spectral bandpass

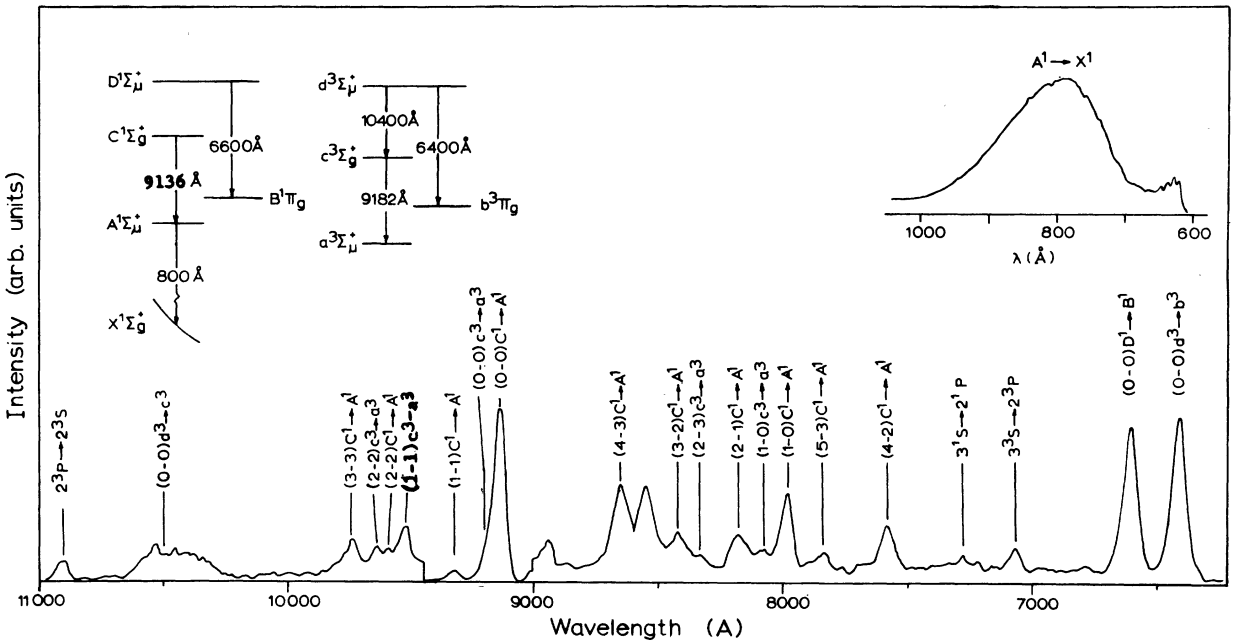

FIG. 1. Emission spectrum of electron-beam–excited superfluid helium and a level diagram for the ground vibrational states of He_2^* that are produced in the liquid.

of about 12 Å. The vacuum-uv (vuv) fluorescence was detected by observing the secondary fluorescence of a sodium-salicylate screen with a EMI 6256 (S-11) phototube.

Measurements of the absolute steady-state intensity as well as the transient decay of each principle emission band were carried out as a function of beam current and temperature for electron beam currents during the pulses of 0.25, 1.0, and 5.0 μA and sample temperatures between 1.4 and 2.08 °K. These experimental conditions do not induce the superfluid helium to boil and they are also below the threshold for the nonvisible local heating phenomenon which is discussed in the preceding paper. The duration of the electron-beam pulse was adjusted to allow sufficient time to achieve steady-state conditions for both the band emission as well as the concentration of metastable states.[10]

A. Steady state and early afterglow

All the principle molecular emission bands exhibit the same qualitative variation with time during and after a pulse of electron-beam excitation. An example of this behavior is shown in Fig. 3. The bands achieve a steady-state intensity during the beam pulse, indicated by the transition rate I^0, and then upon termination of the beam the intensity decays in approximately 10^{-8} sec to smaller value, indicated by I^M, after which it decreases more slowly with a half time that is of the order of milliseconds. The ratios I^M/I^0 were typically in the range 0.1–0.2. The absolute steady-state intensities of the principle emission bands were determined by comparing the fluorescence signal of the excited liquid with the signal observed when the sample was replaced by a tungsten strip-lamp radiance standard. The absolute intensities of the six principle molecular bands for temperatures between 1.68 and 2.08 °K with the liquid at its saturated vapor pressure are given in Table I.

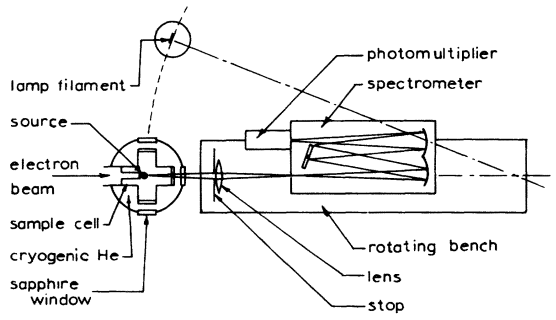

FIG. 2. Experimental arrangement for the optical-emission experiments. The optical bench is pivoted in order to compare the intensities of the liquid-emission bands with a standard lamp.

The tabulated values refer to 1 μA of 160 keV electrons stopped in an estimated 0.04 cm^3 of liquid. The over-all uncertainty in the absolute intensity of the infrared bands could be as large as 50%, which includes the uncertainties in the shape and uniformity of the excited liquid. The 800-Å $A^1 \rightarrow X^1$ band has an additional uncertainty of a factor of 2 arising from the calibration of the sodium salicylate wavelength shifter. The relative intensities of any given band as a function of temperature is estimated to be 10% with the relative intensities of different bands at the same temperature having an additional uncertainty of about 5% due to the standard lamp. The details of the absolute intensity measurements and the associated calculations are described elsewhere.[11] The steady-state intensities of all bands was found to be linearly dependent upon the beam current. The results in Table I indicate a slight decrease of the intensities with decreasing temperature. The $A\,^1\Sigma \rightarrow X\,^1\Sigma$ uv continuum is by far the most intense emission of the excited liquid, and furthermore the radiative transition $C\,^1\Sigma \rightarrow A\,^1\Sigma$ does not by any means account for the population of the $A\,^1\Sigma$ state.

The relative steady-state intensities of the principle molecular bands along with the $2\,^3S \rightarrow 2\,^3P$ and $2\,^3P \rightarrow 2\,^3S$ atomic lines were also measured as a function of pressure between SVP and 25 atm. We find that the intensities of the atomic and molecular emissions decrease exponentially with increasing pressure, in some cases decreasing by as much as several orders of magnitude between

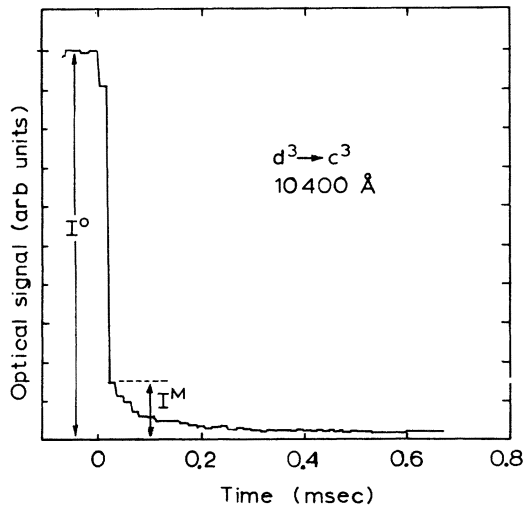

FIG. 3. Typical afterglow decay of emission bands of electron-beam–excited liquid helium showing the early and late afterglow behavior. I^0 is the steady-state intensity and I^M is the contribution to the steady-state intensity which is due to the bimolecular destruction of $He_2(a\,^3\Sigma)$ metastable molecules.

TABLE I. Absolute intensities of the major (0-0) molecular emission bands of electron-beam–excited superfluid helium at the indicated temperatures. The intensities are given in photons/(sec/ $cm^3/\mu A$) of 160-KeV electron beam current stopped in 0.04 cm^3 of liquid.

λ_0(Å)	T (°K)	I^0 ($sec^{-1}cm^{-3}\mu A^{-1}$)
6400	2.08	4.50×10^{13}
	1.89	4.24×10^{13}
	1.79	3.47×10^{13}
	1.68	3.58×10^{13}
6600	2.08	3.60×10^{13}
	2.05	3.43×10^{13}
	1.94	3.47×10^{13}
	1.89	3.21×10^{13}
9136	2.08	1.44×10^{14}
	1.89	1.35×10^{14}
	1.79	1.15×10^{14}
	1.68	8.66×10^{13}
9182	2.08	2.26×10^{13}
	1.89	2.23×10^{13}
	1.79	1.44×10^{13}
10400	2.08	3.67×10^{13}
	1.89	3.60×10^{13}
	1.79	3.09×10^{13}
	1.69	2.89×10^{13}
vuv zeroth order	2.08	5.0×10^{17}

SVP and 25 atm. This observation is rather surprising, particularly in view of the fact that the density of the liquid changes by only 20% between SVP and 25 atm.[12] The measured pressure-dependent intensities are summarized in Fig. 4, where the intensity of each band has been normalized to unity at SVP. The sensitivity of the various atomic and molecular emissions to pressure quenching is apparently related to the type of the upper state involved in the transition. For example the pressure-dependent intensities of the (0-0) $c\,^3\Sigma \rightarrow a\,^3\Sigma$, (0-0) $C\,^1\Sigma \rightarrow A\,^1\Sigma$, and $2\,^3P \rightarrow 2\,^3S$ transitions are all within the band indicated in Fig. 4, and these transitions are all similar in that the upper state can be characterized by a P-type orbital excited electron.[13] On the other hand, the remainder of the curves in Fig. 4, all of which have different slopes and are outside the P-type band, indicate the intensities of emission from S-type orbital upper states. The intensity of the 800-Å continuum appears to be independent of pressure. It should be noted also that the ratio of the intensities $d^3 \rightarrow b^3$ and $d^3 \rightarrow c^3$ (Curves 4 and 2 in Fig. 4) is pressure dependent even though the upper state is the same for both transitions.

We interpret the results in Fig. 4 as evidence of pressure-induced destruction of the higher excited states as opposed to possible pressure-dependent production rates for these states. Our results indicate that the two lowest states $A\,^1\Sigma$ and $a\,^3\Sigma$ are populated at pressure-independent rates, and that a pressure-dependent production mechanism is unlikely. Since these rates are many orders of magnitude greater than that due to radiative cascade, the production of the two lowest states could be related to the pressure dependent nonradiative destruction of higher states.[10] Direct evidence for the quenching of the higher

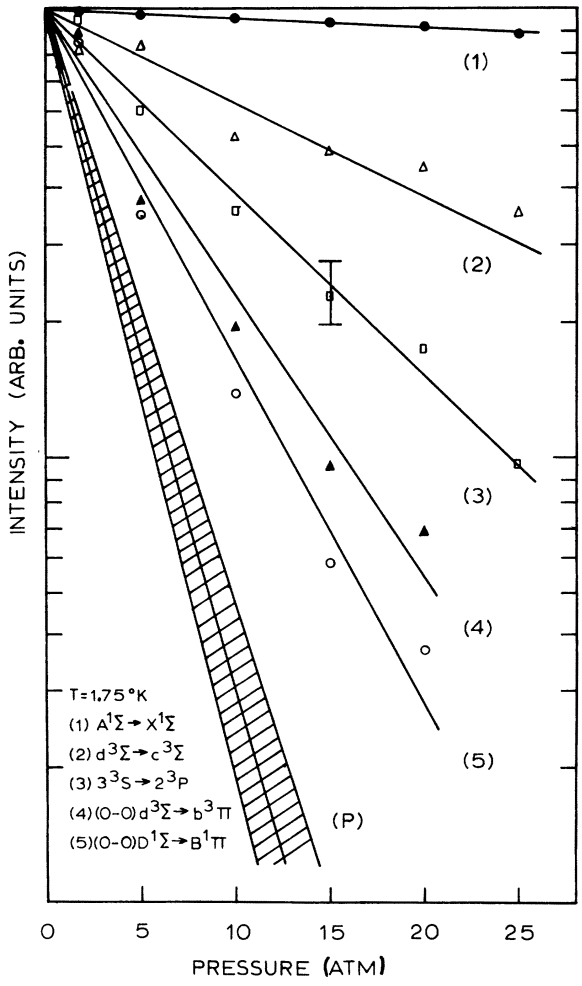

FIG. 4. Relative steady-state intensities of atomic and molecular emissions of excited liquid helium vs pressure. The intensities have been normalized to unity at saturated vapor pressure. The hatched area labeled P indicates the quenching of the (0-0) $a^3\Sigma \rightarrow a^3\Sigma$, (0-0) $C^1\Sigma \rightarrow A^1\Sigma$, and $2\,^3P \rightarrow 2\,^3S$ bands, all of which have a P-type orbital excited electron in the upper state. The remaining curves refer to transitions for which the upper state can be characterized by an S-type orbital electron.

excited states could be obtained by measuring the fluorescence decay times during the early afterglow. Unfortunately, the response time of our present optical detection system is too long for these measurements. Nevertheless, we were able to establish an upper limit of 20 nsec for the decay times of the $c^3 \rightarrow a^3$ and $C^1 \rightarrow A^1$ transitions. Since an oscillator strength of unity would imply a lifetime of about 13 nsec for these transitions, the upper limit of 20 nsec is much shorter than the expected radiative lifetime and thus the C states appear to be nonradiative quenched. Further evidence for the quenching of the $c\,^3\Sigma$ state is indicated by the pressure dependence of the intensity ratio $d^3 \rightarrow c^3/c^3 \rightarrow a^3$ which increases from unity at SVP to roughly 100 at 15 atm.

The quenching of excited states in liquid systems is a well known phenomenon. However, the strong pressure dependence observed in the liquid-helium experiments is an unexpected result. For example, the effects of pressure on the fluorescence of most liquids is due to either the changes in density or index of refraction (a small effect), or to the pressure dependence of the viscosity (or diffusion coefficient) which influences the excitation transfer rates between excited states and other solute molecules.[14] However, the pressure effects in the liquid helium case are too large to be explained by changes in the macroscopic properties of the fluid, and except for the very-long-lived $a\,^3\Sigma$ metastable molecules there is no evidence for a destruction mechanism that is related to the transport properties of the liquid.[10] We conclude that the pressure quenching of the liquid-helium fluorescence must be related to the microscopic interaction between the excited states and the immediately surrounding liquid.[15] The quenching mechanism could involve the formation of a complex of atoms which ultimately results in the production of either the $A\,^1\Sigma$ or $a\,^3\Sigma$ states depending upon the spin quantum number of the original state. In fact, such a process has been invoked previously to account for the destruction of the $2\,^1S$ and $2\,^3S$ atomic metastable states in the liquid.[5, 10]

Our investigation of the steady-state and early afterglow behavior of the atomic and molecular fluorescence of electron beam excited liquid helium has established that all but the lowest spin singlet and spin triplet molecular states are quenched by the surrounding liquid. The characteristic quenching times are of the order of less than 10 nsec. Additional experiments are required to establish the nature of this quenching phenomenon as well as to study the production mechanisms. The fluorescent decay times of the various transitions should be examined as a function of pressure and density in both the liquid and dense-gas phases of helium. We hope to conduct experiments of this type in the near future.

B. Late afterglow

The late afterglow of electron-bombarded superfluid helium is the time period which begins approximately 20 nsec after the termination of the beam pulse, indicated by the transition rate I^M in Fig. 3, and extends for times of the order of several milliseconds during which the intensity of the fluorescence decays toward zero. With our experimental conditions this fluorescence signal consists of separated single photon events, and the experiment must determine the distribution of emitted photons as a function of time for each of the principle molecular emission bands. The apparatus used to record the data is shown schematically in Fig. 5. Standard pulse-height discrimination techniques are used to obtain acceptable photomultiplier pulses, and then each of these pulses is converted into a current pulse representing a predetermined amount of total charge by using a constant current amplifier that is gated by a variable one-shot multivibrator. After this preparation, the time-dependent distribution of afterglow photoemissions is represented by the same distribution of charge pulses. These signals were recorded by using a PAR waveform eductor that was modified so that each of its 100 identical memory capacitors would function as a scaler. Each memory capacitor corresponds to a time t_i after the electron-beam pulse with all memory units having consecutive and equal channel durations δt. The charge pulses were applied directly to the memory "bus-bar" of the eductor; this required bypassing the input amplifier and time constant circuits of the instrument. In this way the eductor functions as a 100 channel multiscaler since each detected photon is represented as a known quantity of charge deposited on one or another memory capacitor depending upon the time of emission. After observing n repetitive afterglow decay signals, the voltage V_i appearing on a given memory capacitor is given by

$$V_i = I_i\, \delta t\, n(Q/C),$$

where I_i is the photon counting rate at time t_i, Q is the charge deposited for each count, and C is the capacitance of the memory unit. Separate calibration measurements established that V_i was linearly proportional to I_i and n and independent of both t_i and δt for counting rates between 10^2 and 10^5/sec to within 4%, as long as the over-all stored signal did not exceed 80% of the maximum dynamic range of the eductor. The afterglow emission signals re-

corded with this system were scaled in order to represent the true emission rates by determining the ratio I^M/I^0 for each band and then comparing the steady-state signals measured in the multi-scaling mode with the absolute measurements shown in Table I.

The late afterglow of electron-beam–excited superfluid helium is evidence of a mechanism which slowly populates excited states of the helium molecule. There are two candidates for this mechanism: One is the slow recombination of ions which could take place in the bulk liquid, and the other is the bilinear destruction of the long-lived $He_2(a\,^3\Sigma_u^+)$ metastable states which are produced by the electron beam. Both of these mechanisms are bilinear in nature and they would result in the same qualitative behavior of the afterglow fluorescence. However, we will present quantitative measurements which indicate that the delayed fluorescence of the liquid is due to the bilinear loss of metastable molecules. If, for the moment, we assume that the metastable molecules is the important energy storage mechanism, then the delayed population of the higher excited states would be described by the reaction

$$\begin{aligned} a\,^3\Sigma_u^+ + a\,^3\Sigma_u^+ &\rightarrow He_4^* \rightarrow A\,^1\Sigma_u^+ + 2He \quad \text{(with probability } f_A\text{)}, \\ &\rightarrow C\,^1\Sigma_g^+ + 2He \quad \text{(with probability } f_c\text{)}, \\ &\rightarrow c\,^3\Sigma_g^+ + 2He \quad \text{(with probability } f_c\text{)}, \\ &\text{etc.} \end{aligned} \tag{1}$$

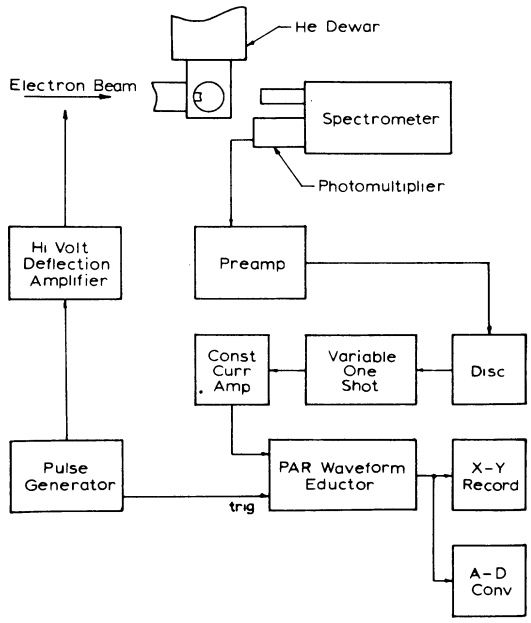

FIG. 5. Schematic of counting system used for late afterglow measurements.

The exact nature of the intermediate complex He_4^* and whether or not an ionic species is formed as an intermediate step is not known, nor are all the possible products of this reaction known. Nevertheless, the net result is a production rate for a given excited molecule which is proportional to the loss rate of metastable molecules multiplied by the factor $f^i/2$, where f^i is the probability of producing the ith excited state during the reaction. If one considers the concentration N_i of the ith excited state of He_2 during the afterglow time period, then the delayed production mechanism suggested by Eq. (1) would imply that the concentration of this excited state would obey an equation of the form

$$\frac{dN_i}{dt} = +\frac{f^i \alpha M^2}{2} - (\nu_{ij} + \nu_{ik} + \nu_q)N_i\,, \tag{2}$$

where αM^2 is the rate at which metastable molecules are destroyed during the afterglow, $(\nu_{ij} + \nu_{ik})$ represents the rates of optical de-excitation of the ith level to two supposed lower states, and ν_q is included to account for possible nonradiative quenching of the state under consideration. Equation (2) is sufficiently general to describe the molecular emission bands that we will discuss. During the late afterglow the production of excited molecular states is expected to proceed very slowly compared to any of the optical transition rates; thus a quasisteady state will exist during which $dN_i/dt \approx 0$. In this case one may solve for $\nu_{ij}N_i$, which is the measured instantaneous emission signal I_{ij} in transitions/sec/cm^3 referred to 1 μA of electron-beam excitation. Thus the observed afterglow-emission signal is expected to obey the relation:

$$I_{ij} = [\nu_{ij}/(\nu_{ij} + \nu_{ik} + \nu_q)](f^i \alpha M^2/2)\,. \tag{3}$$

It is shown in the previous paper that the concentration of metastable molecules during the afterglow decays according to the relation:

$$M(t) = M_0/(1 + \alpha M_0 t)\,, \tag{4}$$

where M_0 is the initial concentration of metastable states, α is the temperature-dependent reaction coefficient for the bilinear destruction of these states, and t is the time after the end of the electron beam pulse. Combining Eqs. (3) and (4) with some algebraic manipulation, it can be shown that the inverse square root of the observed afterglow fluorescence should vary linearly with time as described by

$$(I_{ij})^{-1/2} = (I_{ij}^M)^{-1/2} + m_{ij}t\,, \tag{5}$$

where the initial late afterglow intensity extrapolated to zero time is given by

$$(I_{ij}^M)^{-1/2} = [(\nu_{ij} + \nu_{ik} + \nu_q)/\nu_{ij}](2/f^i)^{1/2}\alpha^{-1/2}M_0^{-1}, \tag{6a}$$

$$(I_{ij}^M)^{-1/2} = [(\nu_{ij} + \nu_{ik} + \nu_q)/\nu_{ij}]^{1/2}(2/f^i)^{1/2}(KI)^{-1/2}. \tag{6b}$$

Equation (6b) follows from Eq. (6a) due to the relationship $M_0 = (KI/\alpha)^{1/2}$ discussed in the previous paper; K is the coefficient for the production of metastable molecules due to the beam electrons and I is the beam current. The slope in Eq. (5) is given by

$$m_{ij} = [(\nu_{ij} + \nu_{ik} + \nu_q)/\nu_{ij}]^{1/2}(2/f^i)^{1/2}(\alpha)^{1/2}. \tag{7}$$

Our observations of the late time fluorescence of electron-bombarded superfluid helium agree with the model suggested by Eqs. (5)–(7). An example of our results is in Fig. 6, where the inverse square root of the observed $d^3 \rightarrow b^3$ (6400 Å) late afterglow emission is shown for the temperatures of 2.08 and 1.79 °K with beam currents of 0.25, 1.0, and 5.0 μA. The inverse square root of the signal increases linearly with time in agreement with Eq. (5), and the intercept or $(I_{db}^M)^{-1/2}$ varies as the inverse square root of the beam current as suggested by Eq. (6b). Also the slope or m_{db} is independent of the beam current in agreement with Eq. (7). The increase of the slope with decreasing temperature is expected from the temperature dependence of $\alpha^{1/2}$ in Eq. (7) if all the other factors are independent of the temperature.

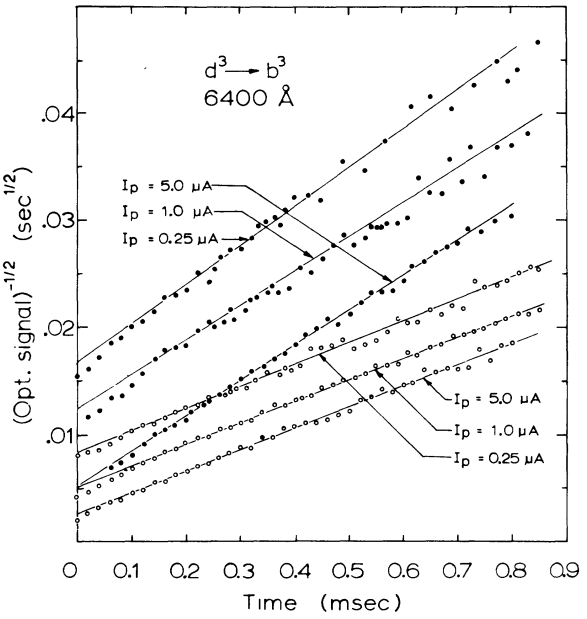

FIG. 6. Inverse square root of the $d^3\Sigma \rightarrow b^3\Pi$ late afterglow intensity vs time. Open circles, for $T = 2.08$ °K; solid dots, for $T = 1.79$ °K. The observed linearity with time of $I_{db}^{-1/2}$ with a slope that is independent of beam current but decreases with temperature is consistent with the model suggested by Eq. (2) of the text.

The afterglow of all the principle molecular bands was fitted to Eq. (5) in order to determine the best intercept and slope for each band. The weighted-least-squares technique of Steinback and Cook was used for this analysis.[16] After this fitting procedure the best slope and intercept for each band was scaled according to the previous measurements of absolute intensities in order to obtain absolute values for these quantities. The results may be discussed more conveniently in terms of the squares of these quantities, which are given by

$$I_{ij}^M = [\nu_{ij}/(\nu_{ij} + \nu_{ik} + \nu_q)](f^i/2)(KI) \tag{8a}$$

and

$$m_{ij}^2 = (KI/I_{ij}^M)\alpha = \alpha^2 M_0^2/I_{ij}^M. \tag{8b}$$

The squared slopes m^2 are plotted as a function of the inverse temperature for the $A^1 \rightarrow X^1$, $c^3 \rightarrow a^3$, $d^3 \rightarrow c^3$, and $C^1 \rightarrow A^1$ molecular emission bands in Fig. 7. The observed temperature dependence of m^2 for each of these bands is the same as the temperature dependence of the bilinear reaction coefficient $\alpha(T)$. This result and the form of Eq. (7) imply that the optical and nonradiative transition rates, as well as the probability factors f, are independent of the temperature. Furthermore, Eq. (6b) indicates that the initial intensity of the late afterglow emission I_{ij}^M should be independent of the temperature. As shown in Fig. 8, this is essentially the case, except for perhaps the initial intensity of the $A^1 \rightarrow X^1$ transition which increases slightly as the temperature is reduced from 2.08 to 1.4 °K.

The qualitative agreement between the data shown in Figs. 6–8 and the expected behavior indicated by Eqs. (1)–(7) firmly establish the bilinear nature of the mechanism which results in the late afterglow fluorescence of the liquid. However, quantitative comparisons are necessary in order to demonstrate that the important mechanism is the bilinear destruction of the metastable molecules. For example, even though the temperature dependence of the squared slopes m^2 suggests the importance of the metastable molecules, one would also expect roughly this temperature dependence to characterize the bilinear recombination of ions in the liquid.[17] On the other hand, Eqs. (6a) and (7) indicate that if one forms the product of the measured

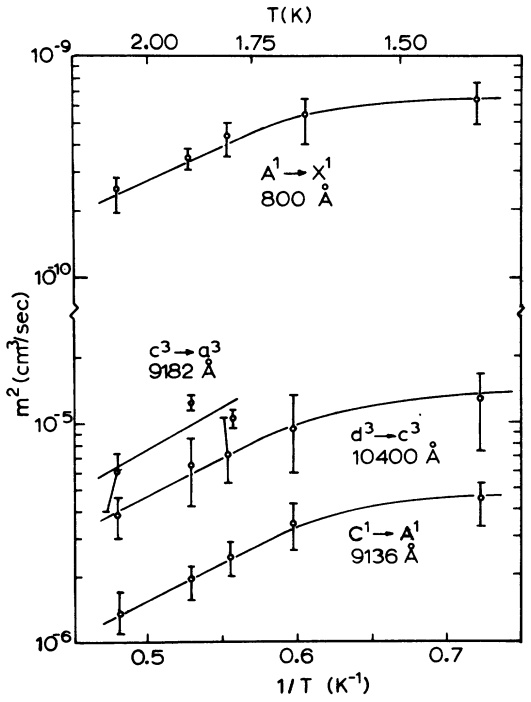

FIG. 7. The squared slopes m^2, as defined in Eq. (8b), vs inverse temperature for the $A^1 \rightarrow X^1$, $c^3 \rightarrow a^3$, $d^3 \rightarrow c^3$, and $C^1 \rightarrow A^1$ molecular-emission bands. The resulting curves indicate a temperature dependence that is the same as $\alpha(T)$, which implies that the formation probabilities and de-excitation rates as discussed in Eqs. (1) and (2) are essentially independent of temperature.

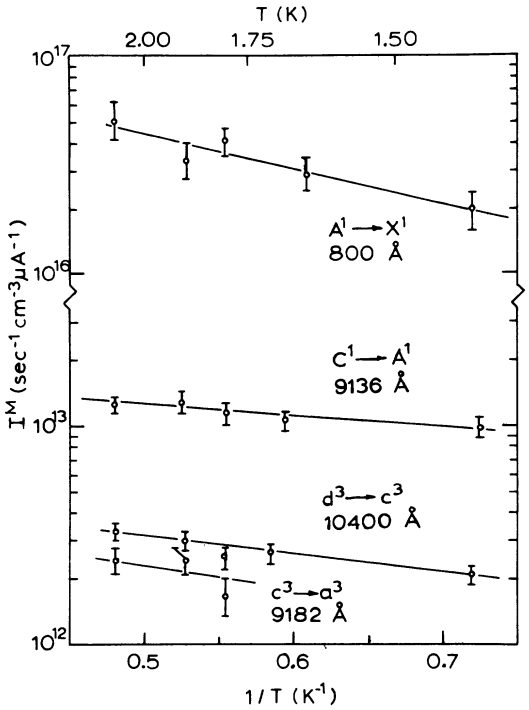

FIG. 8. The initial intensities I^M_{ij} of the vacuum-uv and infrared bands resulting from the bimolecular destruction of $a^3\Sigma$ metastable molecules. The observed slight decrease of the I^M with decreasing temperature may reflect a weak temperature dependence of the formation probabilities or de-excitation rates.

quantities $I^M_{ij}m^2$ for each of the different emission bands, the result should have the same numerical value $\alpha^2(T)M_0^2$ in each case. It should be noted that $1/\alpha(T)M_0$ is simply the half-time for the decay of the concentration of $He_2(a^3\Sigma_u^+)$ molecules under given experimental conditions of temperature and beam current. We estimate the value of $\alpha^2(T)M_0^2$ to be about 10^7 sec^{-2} with 1 μA of beam current at 2.08 °K, and evaluating $I^M_{ij}m^2$ from our data we obtain 1.2×10^7, 4×10^7, 5.4×10^6, 1.5×10^7, 2.2×10^7, and 1.4×10^7 sec^{-2} for the $A^1 \rightarrow X^1$, $d^3 \rightarrow c^3$, $C^1 \rightarrow A^1$, $c^3 \rightarrow a^3$, $D^1 \rightarrow B^1$, and $d^3 \rightarrow b^3$ bands, respectively. This quantitative agreement indicates that all of the above states are populated by the same mechanism during the afterglow, and that the mechanism is the bilinear destruction of metastable molecules. The factor of about 3 variation between the largest and smallest of these numbers is felt to be within the over-all experimental uncertainties, particularly in view of the fact that these measurements were carried out over a time span of several months. A second quantitative comparison may be carried out with respect to the $A^1 \rightarrow X^1$ uv transition. In the case of the $A\,^1\Sigma_u^+$ state there is only one optical transition to be considered, and furthermore the nonradiative quenching of the state cannot be important since a very large fraction of the electron beam power (approximately 30%) is converted into uv light. Thus Eq. (6a) reduces to the simple expression

$$I^M_{AX} = (f^A/2)\alpha(T)M_0^2.$$

By using the measured values of I^M_{AX} and $\alpha(T)M_0^2$ which correspond to 1 μA of beam current at 2.08 °K, it can be shown that the probability factor f^A is approximately 2. Clearly a probability greater than one is not reasonable. However, our result of 2 is well within the experimental uncertainties and it indicates that a large fraction of the energy released during the bilinear metastable reactions results in the formation of $A\,^1\Sigma_u^+$ molecules. Furthermore, if one were to use the known ion mobilities in liquid helium and attempted to evaluate f^A on the basis of ionic recombination, the minimum value of f^A is about 10^3.[16] This result is indeed unreasonable and it rules out ionic recombination as the important populating mechanism dur-

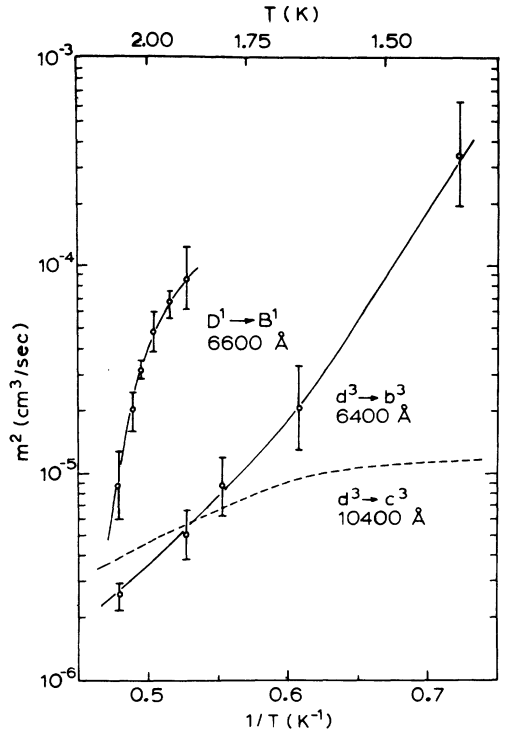

FIG. 9. The squared slopes m^2, as defined in Eq. (8b), vs inverse temperature for the $D^1 \rightarrow B^0$ and $d^3 \rightarrow b^3$ molecular bands compared with the behavior of the $d^3 \rightarrow c^3$ emission band.

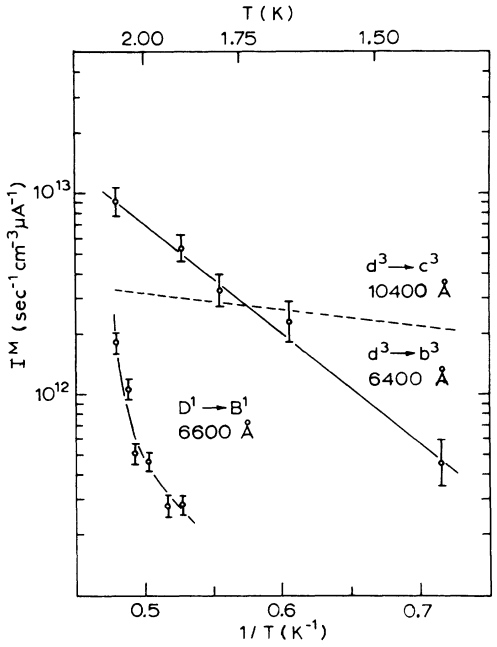

FIG. 10. The initial intensities I_{ij}^M for the $D^1 \rightarrow B^1$ and $d^3 \rightarrow b^3$ molecular bands compared with the behavior of the $d^3 \rightarrow c^3$ band.

ing the late afterglow. It is not possible to obtain reliable estimates of f^i for the other excited states, since the nonradiative quenching rates are unknown, and in the cases where more than one optical transition needs to be considered, the optical transition frequencies are unknown also.

The reader may have noted that the slopes and intercepts for the $D^1 \rightarrow B^1$ (6600 Å) and $d^3 \rightarrow b^3$ (6400 Å) bands have not been included in Figs. 7 and 8. This is because the measured slopes and intercepts for these two bands exhibit an unusual and strong variation with temperature. Our results are shown in Figs. 9 and 10, where the corresponding quantities for the associated $d^3 \rightarrow c^3$ band have been included for comparison. The importance of this observation lies in the fact that the $d^3\Sigma_u^+$ state is the upper state for both of the spin triplet transitions. Equations (6) or (7) may be used to show that for the $d^3 \rightarrow b^3$ and $d^3 \rightarrow c^3$ bands the ratios of either the initial afterglow intensities or the squared slopes depends only upon the ratio of the optical transition rates. In other words, the optical branching ratio is given by

$$I_{db}^M / I_{dc}^M = \nu_{db} / \nu_{dc} ,$$

and our observations indicate that this ratio depends upon the temperature of the surrounding superfluid helium. The observed temperature-dependent branching ratio is very likely related to the details of the interaction between the excited state and the surrounding liquid as is the previously mentioned pressure-dependent quenching phenomenon.[15]

III. SUMMARY

The steady-state and afterglow electron-beam–induced fluorescence of liquid helium has been studied over a wide range of temperatures and pressures. It is shown that the steady-state intensity of the atomic and molecular emissions is influenced by a quenching mechanism which is due to the presence of the surrounding fluid and which depends strongly upon the type of upper state involved in the transition. It has also been shown that the late afterglow fluorescence of liquid helium is due to the bilinear destruction of $He_2(a^3\Sigma)$ metastable molecules.

*Research supported in part by the National Science Foundation.

†Present address: Physics Department, Rice University, Houston, Texas.

‡Present address: Physics Department, University of Texas, Dallas, Texas.

[1]Frank E. Moss and Frank L. Hereford, Phys. Rev. Lett. 11, 63 (1963).

[2]J. Jortner, L. Meyer, S. A. Rice, and E. G. Wilson, Phys. Rev. Lett. 12, 415 (1964).

[3]C. M. Surko and F. Reif, Phys. Rev. 175, 229 (1968).

[4]W. S. Dennis, E. Durbin, Jr., W. A. Fitzsimmons, O. Heybey, and G. K. Walters, Phys. Rev. Lett. 23, 1083 (1969).

[5]M. Stockton, J. W. Keto, and W. A. Fitzsimmons, Phys. Rev. A 5, 372 (1972).

[6]C. M. Surko, R. E. Packard, G. J. Dick, and F. Reif, Phys. Rev. Lett. 24, 657 (1970). See also M. Stockton, J. W. Keto, and W. A. Fitzsimmons, Phys. Rev. Lett. 24, 654 (1970).

[7]M. Stockton and W. A. Fitzsimmons, Bull. Am. Phys. Soc. 17, 454 (1972).

[8]Melvyn R. Fischback, Juey A. Roberts, and Frank L. Hereford, Phys. Rev. Lett. 23, 462 (1969).

[9]J. C. Hill, O. Heybey, and G. K. Walters, Phys. Rev. Lett. 26, 1213 (1971).

[10]J. W. Keto, F. J. Soley, M. Stockton, and W. A. Fitzsimmons, preceding paper, Phys. Rev. A 10, 872 (1974).

[11]The absolute intensity measurements are described in detail in J. W. Keto, Ph.D. thesis, Physics Department, University of Wisconsin (1972) (unpublished). See also R. L. Christiansen and I. Ames, J. Opt. Soc. of Am. 51, 224 (1961).

[12]J. Wilks, *The Properties of Liquid and Solid Helium* (Oxford U. P., London, 1967).

[13]Gerhard Herzberg, *Molecular Spectra and Molecular Structure: I. Spectra of Diatomic Molecules*, 2nd ed. (Van Nostrand, Princeton, N.J., 1950).

[14]See, for example, Henry W. Offen and David T. Phillips, J. Chem. Phys. 49, 3995 (1968); and A. H. Ewald, J. Phys. Chem. 67, 1727 (1963).

[15]W. Steets, A. P. Hickman, and N. F. Lane, Phys. Rev. Lett. (to be published).

[16]Wayne R. Steinback and David M. Cook, Am. J. Phys. 38, 751 (1970).

[17]G. Gareri and F. Gaeta, Nuovo Cimento 20, 152 (1961).